Effective Low-Energy Theory for Correlated Carbon Nanotubes

Reinhold Egger[1] and Alexander O. Gogolin[2]
[1]*Fakultät für Physik, Albert-Ludwigs-Universität, Hermann-Herder-Straße 3, D-79104 Freiburg, Germany*
[2]*Department of Mathematics, Imperial College, 180 Queen's Gate, London SW7 2BZ, United Kingdom*
(Received 12 June 1997)

The low-energy theory for single-wall carbon nanotubes including Coulomb interactions is derived and analyzed. It describes two fermion chains without interchain hopping but coupled in a specific way by the interaction. The strong-coupling properties are studied by bosonization, and consequences for experiments on single armchair nanotubes are discussed. [S0031-9007(97)04654-1]

PACS numbers: 71.10.Pm, 71.20.Tx, 72.80.Rj

The recent discovery of carbon nanotubes [1] has sparked a tremendous amount of activity. Nanotubes are nanoscale particles obtained by wrapping a single layer of graphite into a cylinder. The electronic properties of a (n,m) tube are determined by the integer indices $0 \le m \le n$ of the wrapping superlattice vector, and depending on the choice of m and n, the tube is either a metal, a narrow-gap semiconductor, or an insulator [2]. Experimentally, nanotubes can be produced using the carbon-arc technique [1] or by laser ablation [3] of Co- or Ni-doped graphite targets. The latter method yields metallic (n,n) "armchair" nanotubes with $n = 10$ in rather large quantities, usually deposited in triangular-packed ropes. Remarkably, the first transport measurements on a single 3 μm long $(10,10)$ nanotube have been reported recently [4].

Carbon nanotubes are perfect experimental realizations of one-dimensional (1D) conductors. Interacting 1D electrons usually exhibit Luttinger liquid rather than Fermi liquid behavior characterized by, e.g., the absence of Landau quasiparticles, spin-charge separation, suppression of the electron tunneling density of states, and interaction-dependent power laws for transport quantities [5]. So far non-Fermi liquid behavior has been masked by charging effects due to large contact resistances between the nanotube and the attached leads [4]. Nevertheless, future experiments are expected to reveal the anomalous conductance laws and related phenomena discussed here at higher temperature, suitable gate voltages, or smaller contact resistances.

The low-energy theory for uncorrelated nanotubes has been given by Kane and Mele [6]. Here we extend their approach and incorporate Coulomb interactions among the electrons, focusing on (n,n) tubes where interaction effects are most pronounced [7]. Previously, this problem has only been studied by the perturbative renormalization group (RG) using a weak short-range (Hubbard) interaction [8]. In this Letter, we discuss arbitrary interaction potentials and, in particular, the strong-coupling regime which emerges at low temperatures. This is of importance as the experiments described in Ref. [4] are characterized by long-ranged (unscreened) Coulomb interactions. The low-energy theory found here is equivalent to two spin-$\frac{1}{2}$ fermion chains coupled in a rather special way by the interactions but without interchain single-particle hopping. In that respect, our theory differs from the standard two-chain problem [9,10]. For simplicity, we consider vanishing contact resistances below (the general case will be discussed elsewhere [11]).

The remarkable electronic properties of carbon nanotubes are due to the special band structure of the π electrons in graphite [12,13]. The Fermi surface consists of two distinct Fermi points $\alpha\vec{K}$ with $\vec{K} = (4\pi/3a, 0)$ and $\alpha = \pm$; see Fig. 1. Here the x axis points along the tube direction and the circumferential variable is $0 \le y \le 2\pi R$, where $R = \sqrt{3}\,na/2\pi$ is the tube radius. The lattice constant is $a = 2.46$ Å. Since the basis of graphite contains two carbon atoms, there are two sublattices $p = \pm$ shifted by the vector $\vec{d} = (0,d)$ (where $d = a/\sqrt{3}$), and hence two degenerate Bloch states $\varphi_{p\alpha}(x,y)$ at each Fermi point $\alpha\vec{K}$. We follow Ref. [13] and choose these states separately on each sublattice such that they vanish on the other (note that $K_y = 0$),

$$\varphi_{p\alpha}(x,y)\varphi_{-p\alpha'}(x,y) = 0\,,$$

$$\varphi_{p\alpha}(x,y) = \frac{\exp(-i\alpha K_x x)}{\sqrt{2\pi R}}\,.$$

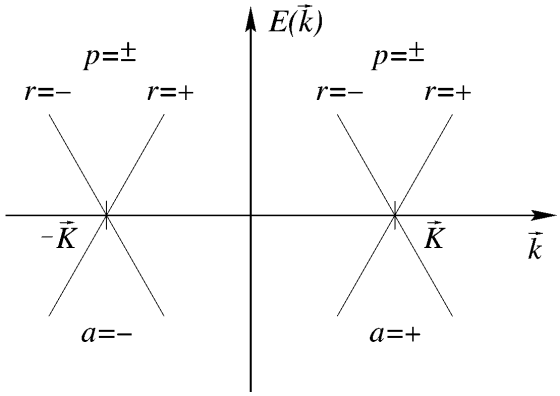

FIG. 1. Low-energy band structure of graphite. Fermi points are labeled by $\alpha = \pm$, and sublattices $p = \pm$ combine to build right and left movers ($r = \pm$).

 0031-9007/97/79(25)/5082(4)$10.00

At low-energy scales, the electron operator for spin $\sigma = \pm$ can be expanded in terms of the Bloch waves [6,13],

$$\Psi_\sigma(x,y) = \sum_{p\alpha} \varphi_{p\alpha}(x,y)\psi_{p\alpha\sigma}(x)\,. \tag{1}$$

Quantization of transverse motion gives the wave function $\chi(y) = \exp(iMy)$ with the "mass" M specified in Ref. [6]. Therefore $\chi = 1$ for armchair tubes ($M = 0$); see Eq. (1). Excitation of other transversal bands costs the energy $\approx 10\ \mathrm{eV}/n$, and hence a 1D situation arises. The conditions for the low-energy regime are met even at room temperature for $(10,10)$ nanotubes. Neglecting Coulomb interactions, the Hamiltonian is [6,13]

$$H_0 = -v \sum_{p\alpha\sigma} p \int dx\, \psi^\dagger_{p\alpha\sigma}\partial_x\psi_{-p\alpha\sigma}\,, \tag{2}$$

where $v \simeq 8 \times 10^5$ m/sec is the Fermi velocity.

Let us now examine Coulomb interactions mediated by a (possibly screened) potential $U(x - x', y - y')$. Electrons trapped in nonpropagating orbitals can be incorporated in terms of a dielectric constant κ, but free charge carriers in nearby gates could lead to an effectively short-ranged potential. For the experiments of Ref. [4], one has an unscreened Coulomb interaction, and the dielectric constant can be estimated as $\kappa \approx 1.4$ [14]. From Eq. (1) the interaction contribution reads

$$H_I = \frac{1}{2}\sum_{pp'\sigma\sigma'}\sum_{\alpha_1\alpha_2\alpha_3\alpha_4}\int dx\,dx'\; V^{pp'}_{\{\alpha_i\}}(x - x') \times \psi^\dagger_{p\alpha_1\sigma}(x)\psi^\dagger_{p'\alpha_2\sigma'}(x')\psi_{p'\alpha_3\sigma'}(x')\psi_{p\alpha_4\sigma}(x) \tag{3}$$

with the 1D interaction potentials

$$V^{pp'}_{\{\alpha_i\}}(x - x') = \int_0^{2\pi R} dy\,dy'\,\varphi^*_{p\alpha_1}(x,y)\varphi^*_{p'\alpha_2}(x',y') \times U(x - x', y - y' + pd\delta_{p,-p'}) \times \varphi_{p'\alpha_3}(x',y')\varphi_{p\alpha_4}(x,y)\,. \tag{4}$$

Here intersublattice interactions involve the shift vector $\vec{d} = (0,d)$. It is natural to distinguish three processes associated with the Fermi points $\alpha = \pm$. First, we have "forward scattering" (αFS) where $\alpha_1 = \alpha_4$ and $\alpha_2 = \alpha_3$. Second, we have "backscattering" (αBS) with $\alpha_1 = -\alpha_2 = \alpha_3 = -\alpha_4$. Finally, at half-filling there is an additional "umklapp" process characterized by $\alpha_1 = \alpha_2 = -\alpha_3 = -\alpha_4$. These processes are different from the conventional ones [5] since they do not necessarily mix right- and left-moving branches but rather involve different Fermi points; see Fig. 1.

Let us start with αFS. We first define

$$V_0(x) = \int_0^{2\pi R}\frac{dy}{2\pi R}\int_0^{2\pi R}\frac{dy'}{2\pi R}\,U(x,y - y')\,, \tag{5}$$

whence from Eq. (4) the $\{\alpha_i\}$-independent 1D potential reads $V^{pp'}_{\alpha\mathrm{FS}}(x) = V_0(x) + \delta_{p,-p'}\delta V_p(x)$ with

$$\delta V_p = \int_0^{2\pi R}\frac{dydy'}{(2\pi R)^2} \times [U(x,y - y' + pd) - U(x,y - y')]\,.$$

The correction δV_p measures the difference between intra- and intersublattice interactions. Because of the periodicity of the y integrals, expanding in powers of d implies $\delta V_p(x) = 0$. Since the potential V_0 does not discriminate among sublattices, the resulting αFS interaction couples only the total 1D charge densities,

$$H^{(0)}_{\alpha\mathrm{FS}} = \frac{1}{2}\int dx\,dx'\,\rho(x)V_0(x - x')\rho(x')\,, \tag{6}$$

with $\rho(x) = \sum_{p\alpha\sigma}\psi^\dagger_{p\alpha\sigma}\psi_{p\alpha\sigma}$. For an unscreened Coulomb interaction ($a_0 \simeq a$),

$$U(x,y) = \frac{e^2}{\kappa\sqrt{a_0^2 + x^2 + 4R^2\sin^2(y/2R)}}\,, \tag{7}$$

the potential (5) becomes

$$V_0(x) = \frac{2e^2}{\kappa\pi\sqrt{a_0^2 + x^2 + 4R^2}}\,K\!\left(\frac{2R}{\sqrt{a_0^2 + x^2 + 4R^2}}\right)$$

with the complete elliptic integral of the first kind $K(z)$. The Fourier transform $V_0(k)$ for $|kR| \ll 1$ is reminiscent of a 1D quantum wire [5],

$$V_0(k) = (e^2/\kappa)[2|\ln(kR)| + \pi\ln 2]\,. \tag{8}$$

For $|x| \gg a$, the above continuum argument leading to $\delta V_p(x) = 0$ safely applies. However, for $|x| \le a$, an additional αFS term beyond Eq. (6) arises due to the hard core of the Coulomb interaction,

$$H^{(1)}_{\alpha\mathrm{FS}} = -f\int dx\sum_{p\alpha\alpha'\sigma\sigma'}\psi^\dagger_{p\alpha\sigma}\psi^\dagger_{-p\alpha'\sigma'}\psi_{-p\alpha'\sigma'}\psi_{p\alpha\sigma} \tag{9}$$

with $f/a = \gamma e^2/R$. Evaluating $\delta V_p(x = 0)$ on the wrapped graphite lattice using Eq. (7) yields

$$\gamma = \frac{\sqrt{3}\,a}{2\pi\kappa a_0}\left[1 - \frac{1}{\sqrt{1 + a^2/3a_0^2}}\right] \approx 0.1\,. \tag{10}$$

Next we discuss αBS contributions. Since Eqs. (3) and (4) involve a rapidly oscillating factor $\exp[2iK_x(x - x')]$, these are local processes which do not resolve sublattices,

$$H_{\alpha\mathrm{BS}} = \frac{b}{2}\int dx\sum_{pp'\alpha\sigma\sigma'}\psi^\dagger_{p\alpha\sigma}\psi^\dagger_{p'-\alpha\sigma'}\psi_{p'\alpha\sigma'}\psi_{p-\alpha\sigma}\,. \tag{11}$$

Estimating the coupling constant b from Eq. (4) for the unscreened interaction (7) results in $b \approx f$, while for well-screened short-ranged interactions, $b \gg f$. Experimentally, by using additional gates, one can easily tune away from half-filling [4]. Therefore we disregard all umklapp scattering effects in this paper.

To study this effective low-energy model, we employ standard Abelian bosonization [5,10]. For that purpose we first switch to right and left movers ($r = \pm$),

$$\psi_{p\alpha\sigma} = \sum_r \tilde{U}_{pr}\psi_{r\alpha\sigma} \quad \text{where } \tilde{U}^\dagger\sigma_y\tilde{U} = \sigma_z\,,$$

which then allow for straightforward bosonization,

$$\psi_{r\alpha\sigma}(x) = \frac{\eta_{r\alpha\sigma}}{\sqrt{2\pi a}} \exp\Big[iq_F rx + i\frac{\sqrt{\pi}}{2}(\phi_{c+} + r\theta_{c+} + \alpha\phi_{c-} + r\alpha\theta_{c-} + \sigma\phi_{s+} + r\sigma\theta_{s+} + \alpha\sigma\phi_{s-} + r\alpha\sigma\theta_{s-})\Big]. \tag{12}$$

Phase fields for the total and relative ($\delta = \pm$) charge ($j = c$) and spin ($j = s$) channels obey the algebra

$$[\phi_{j\delta}(x), \theta_{j'\delta'}(x')] = -(i/2)\delta_{jj'}\delta_{\delta\delta'}\,\mathrm{sgn}(x - x').$$

Thus $\phi_{j\delta}$ and $\theta_{j\delta}$ are dual fields. Density and current operators can be written in terms of the $c+$ field,

$$\rho(x) = (2/\sqrt{\pi})\partial_x\theta_{c+}(x), \qquad I = (2e/\sqrt{\pi})\partial_t\theta_{c+}(0).$$

The wave vector q_F is related to deviations $\delta\rho = 4q_F/\pi$ of the average electron density from half-filling and can be tuned by gates. Finally, the $\eta_{r\alpha\sigma}$ are Majorana fermions ensuring anticommutation relations among different $r\alpha\sigma$. Since the Hamiltonian contains only the combinations $A_{\pm\pm} = \eta_{r\alpha\sigma}\eta_{\pm r\pm\alpha\sigma}$, these can be represented using standard Pauli matrices. Besides $A_{++} = 1$, we have $A_{+-} = i\alpha\sigma_x$, $A_{-+} = ir\alpha\sigma_z$, and $A_{--} = -ir\sigma_y$. Using Eq. (12), the bosonized expressions then read

$$H_0 = \frac{v}{2}\int dx \sum_{j\delta}[(\partial_x\phi_{j\delta})^2 + K_{j\delta}^{-2}(\partial_x\theta_{j\delta})^2], \tag{13}$$

$$H^{(0)}_{\alpha\mathrm{FS}} = \frac{2}{\pi}\int dx\, dx'\, \partial_x\theta_{c+}(x)V_0(x - x')\partial_{x'}\theta_{c+}(x'), \tag{14}$$

$$H^{(1)}_{\alpha\mathrm{FS}} = \frac{f}{(\pi a)^2}\int dx\, [-\cos(\sqrt{4\pi}\,\theta_{c-})\cos(\sqrt{4\pi}\,\theta_{s-}) - \cos(\sqrt{4\pi}\,\theta_{c-})\cos(\sqrt{4\pi}\,\theta_{s+}) + \cos(\sqrt{4\pi}\,\theta_{s+})\cos(\sqrt{4\pi}\,\theta_{s-})] \tag{15}$$

$$H_{\alpha\mathrm{BS}} = \frac{b}{(\pi a)^2}\int dx\, [\cos(\sqrt{4\pi}\,\theta_{c-})\cos(\sqrt{4\pi}\,\theta_{s-}) + \cos(\sqrt{4\pi}\,\theta_{c-})\cos(\sqrt{4\pi}\,\phi_{s-}) + \cos(\sqrt{4\pi}\,\theta_{s-})\cos(\sqrt{4\pi}\,\phi_{s-})]. \tag{16}$$

Although bosonization of Eq. (2) gives $K_{j\delta} = 1$, interactions renormalize these parameters. In particular, $H^{(0)}_{\alpha\mathrm{FS}}$ can be incorporated into H_0 by putting $K_{c+} = K = 1/\sqrt{1 + 4V_0(k \simeq 0)/\pi v} < 1$, while for all other channels, $K_{j\delta} = \sqrt{1 + f/\pi v} > 1$. For the long-ranged interaction (7), one has $K = \mathrm{const}/\sqrt{|\ln[\max(T, v/L)]|}$ [5] such that at zero temperature, K vanishes in a very long tube. Velocity renormalizations are ignored here as they do not change exponents.

From the perturbative RG equations [11], it follows that around the Gaussian point $f = b = 0$, $H^{(1)}_{\alpha\mathrm{FS}}$ is irrelevant, while $H_{\alpha\mathrm{BS}}$ scales to strong coupling, $b \to \infty$. Let us first examine short-ranged interactions such that $f \ll b$. For $f = 0$, the relative charge and spin channels can be refermionized in terms of four Majorana fermions $\xi_{jR(L)}(x)$. Here $j = 1, 2$ corresponds to $(s-)$, $j = 3, 4$ to $(c-)$, and $R(L)$ denotes the right-/left-moving part. Remarkably, refermionization shows that the last term in Eq. (16) vanishes identically, and we are left with

$$H(c-, s-) = -\frac{i}{2}\sum_{j=1}^{4}\int dx(\xi_{jR}\partial_x\xi_{jR} - \xi_{jL}\partial_x\xi_{jL}) - 2b\int dx(\xi_{3R}\xi_{3L} + \xi_{4R}\xi_{4L})\xi_{1R}\xi_{1L}. \tag{17}$$

The Majorana fermion ξ_2 stays massless, i.e., the $(s-)$ sector carries one massive and one massless branch. This behavior is due to the symmetric appearance of the dual fields θ_{s-} and ϕ_{s-} in Eq. (16) which does not permit complete pinning due to the Heisenberg uncertainty relation [10]. The $(c-)$ sector is fully gapped, and we can put $\theta_{c-} = 0$. The masses of the three massive Majorana fermions $\xi_{1,3,4}$ at this strong-coupling point are approximately equal ($\approx m_b$) and can be estimated from mean-field theory as $m_b \approx \omega_c \exp(-\pi v/\sqrt{2}\,b)$, where $\omega_c = 7.4$ eV is the bandwidth of the π electrons [2]. Correlation functions for the $(s-)$ sector follow from the correspondence between two Majorana fermions and the order/disorder operators of the 2D Ising model [10]. In particular, one has scaling dimension $\eta = 1/8$ for $\sin(\sqrt{\pi}\,\theta_{s-})$ and $\sin(\sqrt{\pi}\,\phi_{s-})$, while correlation functions of $\cos(\sqrt{\pi}\,\theta_{s-})$ and $\cos(\sqrt{\pi}\,\phi_{s-})$ decay exponentially. In the $(c-)$ sector, correlations of $\cos(\sqrt{\pi}\,\theta_{c-})$ show long-range order while all other operators lead to exponential decay.

While $H^{(1)}_{\alpha\mathrm{FS}}$ is irrelevant at $f = b = 0$, it becomes relevant at the new strong-coupling point which therefore describes only an intermediate fixed point. The term $\sim\cos(\sqrt{4\pi}\,\theta_{s+})\cos(\sqrt{4\pi}\,\theta_{s-})$ in Eq. (15) stays marginal, but the two other terms become relevant with scaling dimension $\eta = 1$. Therefore ξ_2 as well as the $(s+)$ field acquires the mass $m_f \approx (f/b)m_b$. At the emerging strong-coupling fixed point, we have long-range order in the operators $\cos(\sqrt{\pi}\,\theta_{s+})$, $\cos(\sqrt{\pi}\,\theta_{c-})$, and $\sin(\sqrt{\pi}\,\phi_{s-})$, with exponential decay in all other operators except those of the $(c+)$ sector.

This analysis for a screened interaction potential predicts that the exponents corresponding to the first (intermediate) strong-coupling point should be observable on temperature scales $m_f < T < m_b$ with a crossover to a regime $T < m_f$ dominated by the true $T = 0$ fixed point. For long-ranged interactions, we have $m_f \approx m_b$, and the intermediate fixed point and the associated crossover phenomenon are then absent [15].

With the strong-coupling solution discussed above, we can now examine temperature-dependent susceptibilities and other experimentally accessible quantities of interest.

At temperatures $T > m_b$, the dominant correlations come from the intersublattice charge-density wave (CDW) and spin-density wave (SDW) operators

$$\hat{O}_{\mathrm{CDW}} \sim \sum_{p\alpha\sigma} \psi^{\dagger}_{p\alpha\sigma}\psi_{-p\alpha\sigma}\,,$$

$$\hat{O}_{\mathrm{SDW}} \sim \sum_{p\alpha\sigma} \sigma\psi^{\dagger}_{p\alpha\sigma}\psi_{-p\alpha\sigma}\,,$$

with $\langle \hat{O}(x)\hat{O}(0)\rangle \sim \cos(2q_F x)x^{-(K+3)/2}$ for both [16]. Because of a larger prefactor, SDW correlations will be more pronounced. For $m_f < T < m_b$, this decay is changed into the slower $x^{-(2K+3)/4}$ law. Both the CDW and SDW correlations decay exponentially at very low temperatures $T < m_f$. However, there is also a $4q_F$ CDW component effectively coming from $\hat{O}^2_{\mathrm{CDW}}$ [10], which leads to a slow $\cos(4q_F x)x^{-2K}$ decay at $T < m_b$. This is in fact the dominant instability at temperatures $T < m_b$ and strong correlations, $K < 1/2$. Remarkably, it is not K_x but q_F which determines the period of all the dominating correlations. Since $aq_F \ll 1$, one has pronounced *ferromagnetic* correlations. This offers an explanation for the ferromagnetic tendencies observed in Ref. [4].

Superconductivity (SC) has been predicted to be quite a robust feature of two-chain models [8–10]. In the nanotube, the dominant SC correlations come from the intrasublattice singlet SC pairing operator

$$\hat{O}_{\mathrm{SC}} \sim \sum_{p\alpha\sigma} \sigma\psi_{p\alpha\sigma}\psi_{p-\alpha-\sigma}\,,$$

while triplet SC plays no role. For $T > m_b$, correlations decay faster than x^{-2}, and for $m_f < T < m_b$, their $x^{-(2/K+3)/4}$ decay is subdominant to the CDW and SDW correlations. Finally, at very low temperatures, $T < m_f$, we obtain $\langle \hat{O}_{\mathrm{SC}}(x)\hat{O}_{\mathrm{SC}}(0)\rangle \sim x^{-1/2K}$. Therefore SC becomes the dominant instability only at very low temperatures and for short-ranged interactions ($K > 1/2$).

The properties of the above strong-coupling points also determine conductance laws. In the absence of impurities, one has perfect conductance quantization, $G = G_0 = 4e^2/h$, and experimentally measured resistances are contact resistances. There are nevertheless various sources for impurities, e.g., structural imperfections, charge defects in the substrate, topological defects (dislocation pairs) [1], or twists [6]. They lead to mass-term-like perturbations [6] of the generic form

$$H_{\mathrm{imp}} = v\int dx\, M(x) \sum_{p\alpha\sigma} \psi^{\dagger}_{p\alpha\sigma}\psi_{-p\alpha\sigma}\,.$$

Assuming a single static pointlike impurity center, in order M^2 the following temperature dependence of the corrections δG to G_0 is found. For $T > m_b$, we obtain $\delta G \sim T^{(K-1)/2}$, which is turned into $\delta G \sim T^{(2K-5)/4}$ at $m_f < T < m_b$. At even lower temperature, $T < m_f$, from perturbation theory in M^2, one would get $\delta G \sim T^{K-2}$. For extremely low temperatures, however, by invoking the usual duality argument [5], this is turned into $G(T \to 0) \sim T^{-2+4/K}$, i.e., a vanishing conductance similar to the Luttinger liquid case. For long-ranged interactions, this leads to a pseudogap behavior at very low temperatures.

To conclude, the effective low-energy theory for correlated single-wall nanotubes has been given. Our theory explains the ferromagnetic tendencies observed in recent experiments and predicts the temperature dependence of various susceptibilities and the conductance in the presence of impurities.

We thank M. H. Devoret, D. Esteve, H. Grabert, and A. A. Nersesyan for helpful discussions. This work has been partly carried out during an extended stay of R. E. at the Imperial College funded by the EPSRC of the United Kingdom.

[1] S. Iijima, Nature (London) **54**, 56 (1991); T. W. Ebbesen, Phys. Today **49**, No. 6, 26 (1996).
[2] N. Hamada, S. Sawada, and A. Oshiyama, Phys. Rev. Lett. **68**, 1579 (1992); J. W. Mintmire, B. I. Dunlap, and C. T. White, *ibid.* **68**, 631 (1992); R. Saito, M. Fujita, G. Dresselhaus, and M. S. Dresselhaus, Appl. Phys. Lett. **60**, 2204 (1992).
[3] A. Thess *et al.*, Science **273**, 483 (1996); J. E. Fischer *et al.*, Phys. Rev. B **55**, R4921 (1997).
[4] S. J. Tans, M. H. Devoret, H. Dai, A. Thess, R. E. Smalley, L. J. Geerligs, and C. Dekker, Nature (London) **386**, 474 (1997).
[5] J. Voit, Rep. Prog. Phys. **57**, 977 (1995).
[6] C. L. Kane and E. J. Mele, Phys. Rev. Lett. **78**, 1932 (1997); C. L. Kane *et al.*, cond-mat/9704117.
[7] Our approach can easily be extended to the general (n, m) case by adding a bulk mass term to Eq. (2).
[8] L. Balents and M. P. A. Fisher, Phys. Rev. B **55**, R11 973 (1997); Y. A. Krotov, D. H. Lee, and S. G. Louie, Phys. Rev. Lett. **78**, 4245 (1997).
[9] F. V. Kusmartsev, A. Luther, and A. A. Nersesyan, JETP Lett. **55**, 692 (1992); M. Fabrizio, Phys. Rev. B **48**, 15 838 (1993); A. M. Finkelstein and A. I. Larkin, *ibid.* **47**, 10 461 (1993); D. V. Khveshchenko and T. M. Rice, *ibid.* **50**, 252 (1994); L. Balents and M. P. A. Fisher, *ibid.* **53**, 12 133 (1996).
[10] H. J. Schulz, Phys. Rev. B **53**, R2959 (1996).
[11] R. Egger and A. O. Gogolin (unpublished).
[12] P. R. Wallace, Phys. Rev. **71**, 622 (1947).
[13] D. P. DiVincenzo and E. J. Mele, Phys. Rev. B **29**, 1685 (1984).
[14] For a $1/|x|$ interaction, the charging energy of a tube of length L is $E_c = e^2 \ln(L/R)/\kappa L$. The experimental value $E_c = 2.6$ meV [4] for $L = 3$ μm leads to $\kappa = 1.4$.
[15] A simple order-of-magnitude estimate for $1/|x|$ interactions puts $m_f \approx m_b$ into the mK range. However, for screened interactions, m_b can be significantly larger.
[16] If $\hat{O}$ has scaling dimension η [i.e., $\langle \hat{O}(x)\hat{O}(0)\rangle \sim x^{-2\eta}$], the corresponding susceptibility $\chi \sim T^{2\eta-2}$.